Nafion coated sulfur–carbon electrode for high performance lithium–sulfur batteries

CrossMark

Qiwei Tang [a], Zhongqiang Shan [a], Li Wang [b], Xue Qin [b,*], Kunlei Zhu [a], Jianhua Tian [a], Xuesheng Liu [c]

[a] School of Chemical Engineering and Technology, Tianjin University, Tianjin 300072, China
[b] School of Science, Tianjin University, Tianjin 300072, China
[c] National Key Laboratory of Science and Technology on Power Sources, Tianjin 300381, China

HIGHLIGHTS

- Nafion coated electrode was prepared by coating nafion solution on the surface.
- Nafion membrane could be formed after thoroughly dried.
- Nafion film has the advantages of cation conductivity and anion inconductivity.
- The applicability of nafion membrane in Li–S battery was confirmed.
- The electrochemical performance of Li–S battery has been greatly improved.

ARTICLE INFO

ABSTRACT

In this paper, a nafion coated electrode is prepared to improve the performance of lithium sulfur batteries. It is demonstrated from a series of measurements that the nafion layer is quite effective in reducing shuttle effect and enhancing the stability and the reversibility of the electrode. When measured under the rate of 0.2 C, the initial discharge capacity of the nafion coated electrode can reach 1084 mAh g^{-1}, with a Columbic efficiency of about 100%. After 100 charge/discharge cycles, this electrode can also deliver a reversible capacity of as high as 879 mAh g^{-1}. Significantly, the charge-transfer resistance of the electrode tends to be reducing after coated with an appropriate thickness of nafion film. The cation conductivity as well as anion inconductivity is considered to be the dominant factor for the superior electrochemical properties.

1. Introduction

Over the past several decades, a substantial amount of research effort has been devoted to developing high performance rechargeable batteries. As a typical example, lithium-ion batteries using high-voltage lithium intercalation compounds as cathode electrode have been commonly studied and used in a series of portable electronic devices such as mobile phones, laptops and digital cameras [1,2]. However, due to the properties of high molecular weight and less electron reaction of these intercalation compounds, the maximum capability of lithium-ion batteries is inherently limited to about 300 mAh g^{-1} and the energy density about 560 Wh kg^{-1} even fully developed, which cannot meet the ever increasing demands for power electric vehicles and plugin hybrid electric vehicles [3–5]. In addition, oxygen could be formed during the over-charge state of ordinary Li ion batteries, which is easy to cause the battery explosion.

Sulfur is a kind of light-weight material, and has the advantages of nature abundance and low cost. When coupled with metallic lithium, sulfur can completely react with lithium to form Li$_2$S, corresponding to a high theoretical gravimetric capacity of 1675 mAh g^{-1} and theoretical energy density of 2600 Wh kg^{-1}, which is almost five times higher than that of current lithium-ion batteries [6–11]. Furthermore, the operating voltage of a Li/S system is 2.1–2.4 V, which makes the battery safer during practical application. Therefore, Li–S batteries are considered as one of the

* Corresponding author. Tel.: +86 (0) 2227406558; fax: +86 (0) 2227404208.
E-mail address: publicly2009@126.com (X. Qin).

most probable candidates to meet the ever increasing demand for high energy storage system. However, the commercial realization of Li−S battery is still difficult due to the following problems: (1) elemental sulfur is an insulator (5×10^{-30} S cm^{-1} at 25 °C), which causes to poor recyclability and low rate capability, (2) the intermediate product of polysulfide Li$_2$S$_x$($4 \leq x \leq 8$)is soluble in electrolyte, which gives rise to a shuttle mechanism and leads to fast capacity fading, (3) the poorly effective contact interface of electrode and electrolyte reduces the utilization of active material [12,13]. In order to address the problems discussed above, a variety of strategies have been attempted, including electrolyte modification, anode protection and the fabrication of porous carbon/sulfur composite [14−20].

Here, we propose a cathode protection approach to enhance the cycle stability and improve the Coulombic efficiency of Li−S batteries by coating nafion membrane on the electrode surface. nafion is a well-known perfluoro ionomer, which has a polytetrafluoro-ethylene PTFE backbone and a perfluoronated side chain [21]. The backbone could keep the membrane stable in electrolyte, and the side chain possesses high cation conductivity and anion inconductivity, making it a widely used separator in fuel cells. There are also some researches demonstrate the feasibility of nafion membrane using in Li-ion batteries and Li−S batteries [22]. Different from the former works which directly use a market available nafion membrane as separator or use nafion as binder, we protect the sulfur cathode by coating nafion solution on the electrode surface and then dry it in air to make a nafion modified electrode. Thickness adjustability of nafion membrane is the advantage for this method. The nafion coating electrode reported in this paper is our primary result on the experiment using this method. It was turned out that a uniform and continuous nafion layer was formed on the surface of active materials after thoroughly dried. This modified electrode are well testified through a series of electrochemical measurement as an effective method to improving the performance of lithium sulfur batteries.

2. Experimental

A calculated S−C composite containing sulfur content of 77 wt% was prepared by a planetary ball-milling method. In detail, 7 g S, 2 g BP2000 (a kind super conductive carbon), 35 ml ethanol, and 45 g agate balls were added into agate container, and then ground in a planetary ball-mill with a rotation speed of 300 r min^{-1}. After milling for 9 h, the slurry was completely dried in an oven at 50 °C for 24 h to obtain S/C composite. The cathode electrode was prepared by mixing S/C composite, acetylene black and polyvinylidene fluoride in a weight ratio of 70:20:10, followed by adding a certain amount of N-methyl-2-pyrrolidinone to form a homogeneously slurry. Then the slurry was cast onto an aluminum foil by a doctor blade, dried at 50 °C for 24 h under vacuum. After that, a certain amount of nafion solution (wt. = 5%) was casted on the surface of the active material, and finally airing at room temperature to make a nafion coated electrode. The coin cells CR2032 were assembled in a glove box filled with high pure Ar. Lithium foil was used as reference and counter electrode. The electrolyte was 1 M bis(tri-fluoromethane)sulfonamide lithium salt dissolved in a mixture of dimethoxymethane (DME) and 1,3-dioxolane (DOL) (1:1 by volume). A type of microporous polypropylene (Celgard 2300) was used as the separator. After 100 cycles the cells were also deassembled in the same glove box.

The morphologies of the electrode before and after nafion coating as well as after 100 cycles were characterized by scanning electron microscopy (SEM, HITACHI, S-4800). Infrared spectra were recorded on a BIO-RAD 3000 infrared spectrophotometer in the range of 4000−700 cm^{-1} using the KBr pellet technique. ^{1}HNMR

spectra was recorded at 25 °C on a Varian INOVA 500 MHz spectrometer using CDCl$_3$ as solvent. All of the electrochemical measurements were carried out at room temperature. Galvanostatic charge−discharge method was performed on a LAND CT-2001A system at different current densities in the voltage range of 1.5−3 V vs. Li/Li$^+$. Cyclic voltammetry curves of the battery were recorded on LK3200 electrochemical working station (Tianjin Lanlike, China) at a scan rate of 0.1 mv s^{-1}. In addition, electrochemical impedance spectroscopy was recorded on Zahner IM6ex electrochemical workstation using 5 mV of AC amplitude over the frequency range from 1 MHz to 0.1 Hz.

As a comparison, the electrode without nafion film coating was also prepared in the same way and tested under the same condition. The nafion coated electrode was marked as NC-electrode, and the electrode that without nafion coating was marked as UC-electrode.

3. Results and discussions

The typical morphologies of the electrode with and without nafion coating are shown in Fig. 1. It can be clearly seen from Fig. 1a that the pristine electrode are uniformly covered by S−C composite. After coated on nafion solution, a visible nafion layer is homogeneously formed on the active material as shown in Fig. 1b. The thickness of the nafion membrane was obtained through cross-section SEM image. A sandwich structure of nafion membrane-active material-Al foil was observed in Fig. 1c, in which the S−C composite was tightly confined in the space between Al foil and nafion film, and the nafion film is about 10 μm in thickness. This unique structure could not only avoid the active material falling down from the current collector, but also have the advantage of prevent high-order lithium polysulfide from diffusing to lithium electrode due to the ionic selectivity of the nafion membrane, thus alleviating the drawback of shuttle effect. Therefore, both the cycle stability and Columbic efficiency of Li−S battery have a prodigious improvement. In order to examine the morphology changes after charge/discharge process, the sulfur electrode was disassembled in a glove box and watched thoroughly with pure DOL + DME (1:1 by volume) solution. It can be seen from Fig. 1d that except for a little cracks, most of nafion coating remains integrity after electrochemical cycling, implying the stability of the nafion membrane during charge−discharge process in the electrolyte.

For the FT-IR measurement, nafion membrane power was obtained from the surface of NC-electrode by a sand paper polishing method. The FT-IR spectra of nafion solution and the nafion power are shown in Fig. 2. The transmittance bands at 3456 cm^{-1} and 1642 cm^{-1} are attributed to stretching vibration and bending vibration of the −OH group. The peaks at 1230 cm^{-1}, 1135 cm^{-1}, 1059 cm^{-1}, and 982 cm^{-1} are ascribed to the characteristic functional groups in nafion [23]. It is clear that the characteristic transmittance bands of nafion are very week due to the high concentration of water contained in nafion solution. After completely dry, the nafion's characteristic peaks become very strong while the water peak almost disappeared. Most of water has been removed after airing dry, which indicates the applicability of NC-electrode in lithium battery.

We employed an H-type of electrolytic cell with intermediate diaphragm to test the permeability of nafion membrane. The separator was commercial nafion-117 membrane purchased from Dupont. One end of the electrolysis cell is filled with DMSO, and the other end filled with the mixture of DOL and DME solution. After stood for 12 h, we extract a small amount of solution from the side that prior filled with DMSO to do ^{1}HNMR measurement. Fig. 3 shows the ^{1}HNMR spectra of the solution. The peak at 2.596 ppm and 7.265 ppm are corresponds to DMSO and CDCl$_3$, respectively.
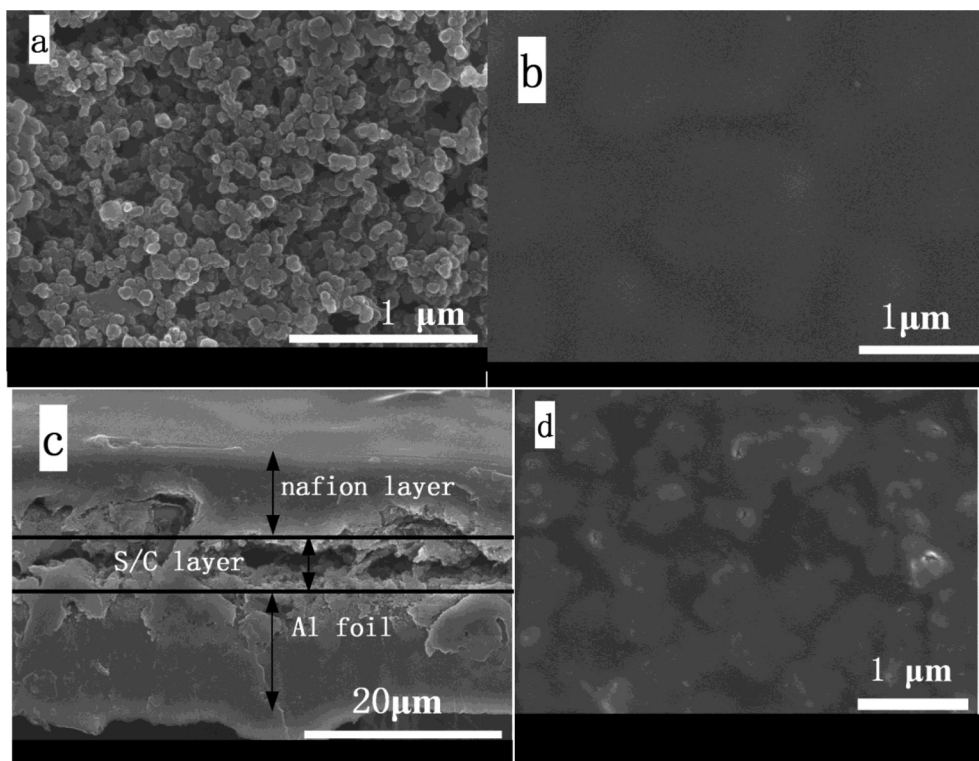
Fig. 1. SEM images of UC-electrode (a), NC-electrode (b), side view of NC-electrode (c), and surface morphology of NC-electrode after 100 cycles (d).

The peaks at 3.369 ppm and 3.519 ppm are related to DME, and the peaks at 3.859 ppm and 4.882 ppm are related to DOL. Both the signals of DOL and DME were detected in the DMSO side. This result reveals that DOL and DME could pass through nafion film.

The electrochemical characteristic of the electrode with and without nafion membrane coating was examined by cyclic voltammetry in the voltage range of 1.5 V–3 V with a scanning rate of 0.1 mv s^{-1}, as shown in Fig. 4. The NC-electrode exhibits nearly the same characteristic reduction peaks as the pure sulfur electrode. Two cathodic peaks are observed at 2.3 V and 2.05 V. The peak at 2.3 V is related to the reduction of elemental sulfur to long chain lithium polysulfides Li_2Sx ($4 \leq x \leq 8$), and the peak at 2.05 V corresponds to the further reduction of these polysulfides to solid Li_2S_2/Li_2S. In the following oxidation process, however, the anodic peaks of NC-electrode are quite different from UC-electrode. As to UC-electrode, there is only one broad oxidation peak appeared at 2.4 V, showing the conversion of Li_2S_2/Li_2S to high-order polysulfides. With the increasing of cycles, the intensity of oxidation peak of UC-electrode decreases increasingly, and the width become broader simultaneously, revealing the electrochemical instability of the active materials within the UC-electrode [6]. In contrast, two oxidation peaks at 2.35 V and 2.45 V were obtained for NC-electrode, which suggests the complete conversion of lithium sulfide to elemental sulfur and corroborates the reversibility electrochemical reaction in the NC-electrode [24,25]. Significantly, there are no changes in the CV peak position or peak intensity for
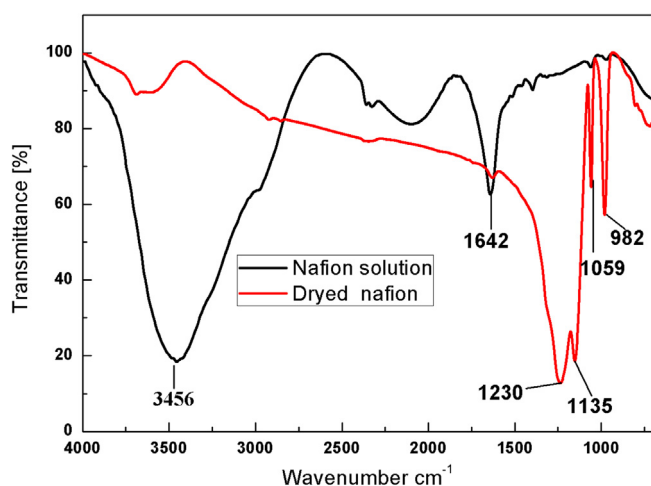

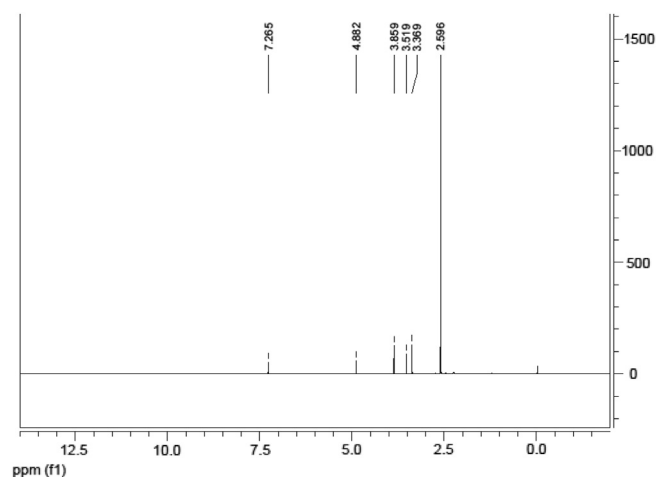**Fig. 2.** FT-IR spectra of nafion solution and nafion film powder.

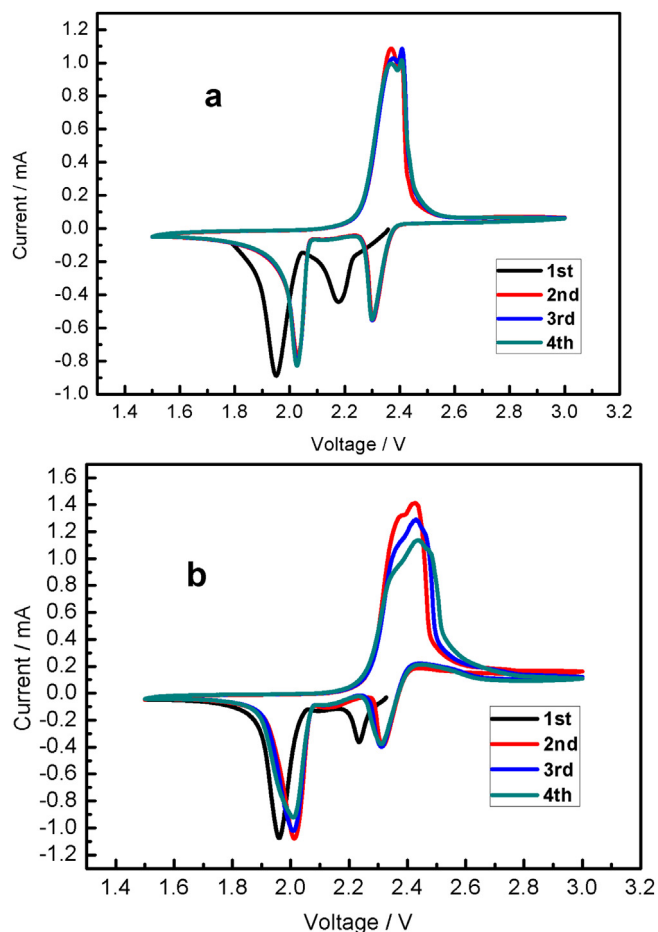

Fig. 3. ^{1}HNMR spectra of DMSO chamber.

Fig. 4. Cyclic voltammograms: (a) NC-electrode; (b)UC-electrode.

Fig. 5. Charge–discharge profiles of UC-electrode (a) and NC-electrode (b).

NC-electrode during cycling, which further confirms the electrochemical stability of the NC-electrode. In the second and following cycles, the reduction peaks of these two kinds of electrode shift from a low voltage to a high voltage, implying that the reaction dynamic of the active material is improved after the initial cycle [18].

In order to gain further insight on the electrochemical performance of the electrodes, galvanostatic charge/discharge was carried out at the current rate of 0.2 C (1 C = 1675 mA g^{-1}) between 1.5 and 3 V. Fig. 5a and b present typical charge/discharge voltage profiles of UC-electrode and NC-electrode, respectively. Consistent with the result from CV measurement, two plateaus exhibit in discharge curve for both UC-electrode and NC-electrode, which can be ascribed to the two step reaction of elemental sulfur with metallic lithium during the discharge process. It is found from Fig. 3a that the UC-electrode delivers a discharge capacity of 896.3 mAh g^{-1} and a charge capacity of 2433.1 mAh g^{-1} in the second cycle, leading to a low Columbic efficiency of 36.8%. The main reason for this phenomenon can be attributed to the "shuttle effect" which is caused by the solubility of higher-order polysulfides that formed on the sulfur electrode during discharge and diffused from S cathode to Li anode where they react directly with metallic lithium to form low-order polysulfides. These reduction products were then diffused back to sulfur electrode to generate higher forms again, thus creating the shuttle mechanism [10]. With the present of this phenomenon, an over-charge is needed to reach full charge condition, thus lading to a huge energy waste. From the charge capacity of 2433.1 mAh g^{-1} and the discharge capacity of
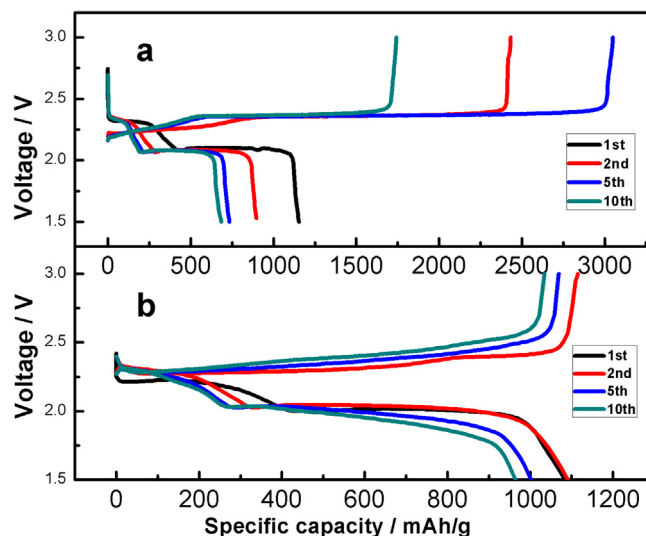
896.3 mAh g^{-1} in the second cycle, we can see that the over-charge is almost ∼171%, meaning more than three-fourths of electric energy is waste. The NC-electrode, by contrast, delivers a discharge capacity of 1091 mAh g^{-1} and a charge capacity of 1115.6 mAh g^{-1} in the second cycle as shown in Fig. 5b. The Columbic efficiency is as high as 97.8%, and the over-charge capacity is only about 2.2%. There are two reasons may account for this enhanced efficiency of NC-electrode. First, nafion membrane possesses high cationic conductivity and anionic insulativity, which allows Li$^+$ to pass through but prevent the polysulfide from penetrating into, thus avoiding the shuttle effect. Second, the nafion coating layer is rigid and stable during the charging/discharging process, which could effectively confine polysulfide tightly between nafion layer and current collector (see in Fig. 1), such that much more polysulfide could be completely converted to Li$_2$S.

The cycle performances of NC-electrode and UC-electrode measured under the current rate of 0.2 C are shown in Fig. 6a. For the UC-electrode, the initial discharge capacity is 1153.3 mAh g^{-1} and the second discharge capacity decreased dramatically to 896.3 mAh g^{-1}, only 77% capacity retention was obtained. The fast
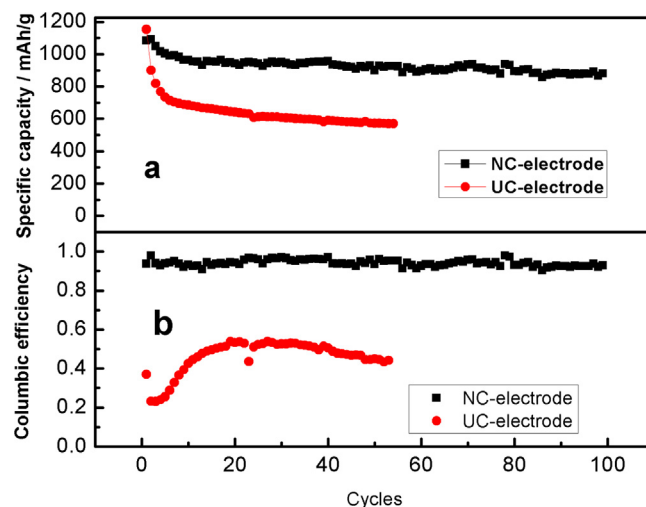

Fig. 6. Cycle performance (a) and Columbic efficiency (b) comparisons of NC-electrode and UC-electrode.

capacity decay in the second cycle can be attributed to the shuttle effect and the irreversible reduction of elemental sulfur to polysulfides that formed in the discharge process and never converted to elemental sulfur in the following charge process. After 55 cycles, the specific capacity of the UC-electrode deduced to 569.6 mAh g^{-1}, which is about 49% of the initial value. On the contrary, the NC-electrode delivers the initial and second discharge capacity of 1084 mAh g^{-1} and 1091 mAh g^{-1} respectively, with a capacity retention of about 100%. Furthermore, the discharge capacity of the NC-electrode can also maintain at 879 mAh g^{-1} even after 100 cycles, corresponding to only 2% capacity decay per cycle during these cycles. This result indicates that the NC-electrode is much stable as compared to UC-electrode, and demonstrates further that the polysulfides are well confined in the space between nofion membrane and current collector by coating nafion solution on the surface of the active materials. To better understand the effect of the nafion coating, the Columbic efficiencies for these different electrodes are compared in Fig. 6b. It is obviously from Fig. 6b that the NC-electrode shows a higher Columbic efficiency of about 95% in the first 80 cycles and a slightly inferior efficiency of 93% in the later stage due to the little crack of the nafion membrane occurred in cycling process as shown in Fig. 1d, while the maximum efficiency of the UC-electrode is only 50%. This further proves that the nafion coating method is quite effective in improving the electrochemical performance of the Li–S batteries. Our observations are different from the results that recently reported in Refs. [26], in which no clear trend or improvement can be confirmed for the nafion coating. The most likely explanation maybe attribute to the inhomogeneous coating and the remained uncovered domains on the active material surface.

The ionic conductivity of nafion was evaluated by using electrochemical impedance spectroscopy (EIS) on a symmetrical two-electrode cell. The conductivity is calculated using the equation (1): $\sigma = d \ A^{-1} \cdot R_b$, where d (50 μm) and A (1.5 cm^2) are denoted separately as the thickness and the area of nafion film, R_b is the resistance of nafion film obtained from the intersection of nyquist plot with abscissa axis. The Li$^+$ transfer number was measured by using the steady-state current method [21], and calculated using the equation (2): $t_{Li}^{+} = I_s(\Delta V - I_0 R_0)/I_0(\Delta V - I_s R_f)$; where R_0 and R_f are the initial and final resistances, I_S is the steady current, ΔV is the applied voltage, I_0 is the initial current calculated from the equation (3): $I_0 = \Delta V/(R_b + R_0)$. The applied voltage was 10 mv. Fig. 7 shows the result of the measurement, in which $R_b = 160 \ \Omega$, $R_0 = 3252\Omega$, $R_f = 3740 \ \Omega$, $I_s = 2.56 \ \mu A$, $\Delta V = 10 \ mv$. It is calculated from the above
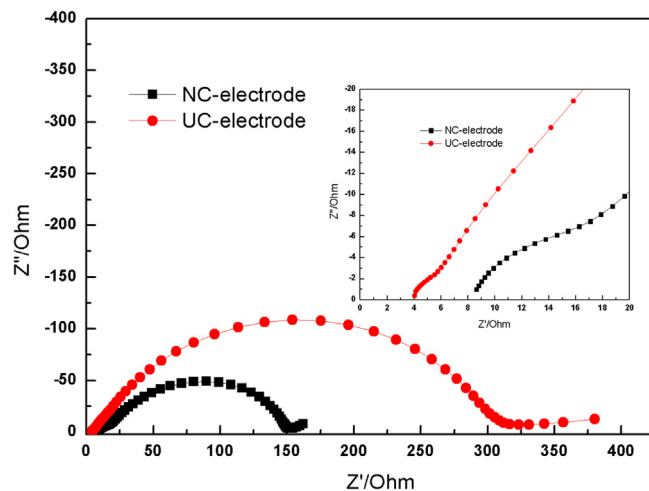
Fig. 8. Nyquist plots for NC-electrode and UC-electrode.

equations that the value of σ and t_{Li}^{+} was 2.08 $\times$ 10^{-5} S cm^{-2} and 0.955, respectively. This result indicates that only Li$^+$ could transport through the nafion film, while anions couldn't. In addition, EIS method was also used to get further insight into the electrochemical process in the electrode. Both the NC-electrode and the UC-electrode was measured under open circuit potential between 1 MKHz and 0.1 Hz.The nyquist plots of NC-electrode and UC-electrode are shown in Fig. 8. The equivalent circuits of these two kinds of electrodes are shown in Fig. 9, where Fig. 9a represents the UC-electrode, and Fig. 9b corresponds to the NC-electrode. As shown in Fig. 9a, the typical equivalent circuit of the UC-electrode consists of one semicircle in high frequency and one straight line in low frequency, corresponding to the interface charge-transfer resistance and Warburg impedance, respectively [27,28]. Different from the UC-electrode, Fig. 9b displays the equivalent circuit consisting of two semicircles and one straight line. The additional semicircle in the high frequency region can be explained as the resistance of the nafion membrane. R_s, R_{ct}, R_1, W_1 and CPE are denoted in the equivalent circuit as solution resistance, electrochemical reaction resistance, nafion film resistance, Warburg impedance and constant phase elemental, respectively. The values of R_s, R_{ct}, R_1 for UC-electrode and NC-electrode are obtained by fitting the equivalent circuit and shown in Table 1. Obviously, the contact resistance (R_s) increases from 4.2 Ω cm^{-2} to 8.7 Ω cm^{-2} with the coating of nafion film due to the low conductivity of the nafion film (2.08 $\times$ 10^{-5} S cm^{-1}).

However, the charge-transfer resistance decreases from 324.9 Ω cm^{-2} to151.4 Ω cm^{-2} with the coating of nafion film. The main reason may be ascribed to the effect that nafion film helps to contain the soluble polysulfide within the space between carbon–sulfur composite particles thus reducing its diffusion to the lithium
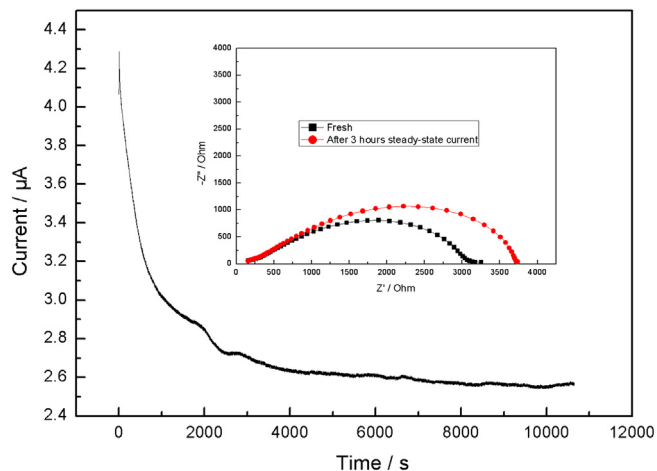

Fig. 7. Current-time profile for Li$^+$ number calculation measured by steady-state current method. Inset is the nyquist plots for the measurement.
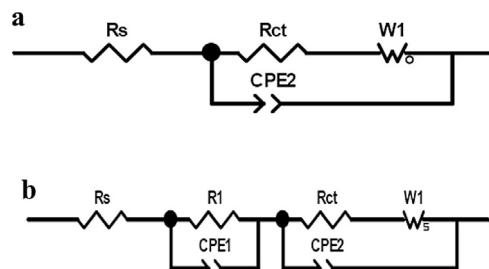

Fig. 9. Equivalent circuit of UC-electrode (a), and NC-electrode (b).

Table 1
The values of R_s, R_1, and R_{ct} for UN-electrode and NC-electrode.

	R_s (Ω cm^{-2})	R_1 (Ω cm^{-2})	R_{ct} (Ω cm^{-2})
UC-electrode	4.2	–	324.9
NC-electrode	8.7	7.0	151.4

anode [17]. Compared to the decreased R_{ct}, the increased R_s and R_1 are negligible, and the overall resistance of the battery tends to be reducing. Considering the low conductivity of nafion film, a suitable thickness range of the film may exist in which the contribution to reducing charge-transfer resistance is far greater than the increased resistance caused by the film itself.

To examine the rate performance of the NC-electrode, the cell was charged and discharged at higher current of 0.5 C, and 1 C, as shown in Fig. 10a. The initial discharge capacity of the NC-electrode at 0.2 C, 0.5 C, and 1 C are 1084 mAh g^{-1}, 968.1 mAh g^{-1} and 639.1 mAh g^{-1}, respectively. After 100 cycles, the discharge capacity of the NC-electrode could remain about 757.3 mAh g^{-1} at 0.5 C rate. When increasing the current density to 1 C, the electrode was still able to deliver a reversible capacity of 602 mAh g^{-1} up to 100 cycles, indicating that the NC-electrode can also be used in the high current rate. The smaller resistance caused by the addition of nafion film maybe the main reason for the high rate performance of the UC-electrode. As an additional reference, the cycle performance of

Li-nafion coated electrode was also examined as shown in Fig. 10b. We employ a previously reported method [22] to perform Li$^+$ exchange of nafion (Li-nafion) before coating. The weight loading of Li-nafion per unit area was similar to the bare nafion. The discharge capacity of the Li-nafion coated electrode at 0.2 C remained at 1052 mAh g^{-1}, which is higher than the capacity retention (934.5 mAh g^{-1}) of NC-electrode at the same cycle. With the current increase to 1 C, the Li-nafion coated electrode could also deliver a higher capacity of 651.9 mAh g^{-1} than that of NC-electrode (595.6 mAh g^{-1}) after 87 cycles. Compared with NC-electrode, the enhanced electrochemical performance of Li-nafion coated electrode can be attributed to the more easily Li$^+$ exchange of Li-nafion coated electrode with the electrolyte than the NC-electrode.

4. Conclusion

In summary, electrode modification method was proposed in this paper to improve the electrochemical performance of lithium–sulfur battery. A nafion coated electrode was prepared by coating nafion solution on the surface of active material. The unique structure of nafion polymer allows the penetration of lithium ion into while prevent polysulfide anions from passing through, which could effectively decreases the shuttle phenomenon and the loss of active material. SEM observation shows the nafion membrane is homogeneous and integrated before cycling, however a little crack was obtained after a long time of circulation, probably due to the expansion of sulfur upon cycling. Even if such a crack phenomenon exists, the NC-electrode can also exhibit a reversible capacity of 1091 mAh g^{-1} in the initial cycle and 879 mAh g^{-1} even after 100 cycles, which is much higher than UC-electrode, demonstrating our method is quite effective in improving the performance of Li–S batteries.

Acknowledgments

Fig. 10. Cycle performances of the NC-electrode (a), and Li-nafion coated electrode (b) at different rates.

References

[1] J.M. Tarascon, M. Armand, Nature 414 (2001) 357–359.
[2] Y. Yang, M.T. Mcdowell, A. Jackson, J.J. Cha, S.S. Hong, Y. Cui, Nano Lett. 10 (2010) 1486–1491.
[3] B. Zhang, X. Qin, G.R. Li, X.P. Gao, Energy Environ. Sci. 3 (2010) 1531–1537.
[4] H.L. Wang, Y. Yang, Y.Y. Liang, L.F. Cui, H.S. Casalongue, Y.G. Li, G.S. Hong, H.J. Dai, Y. Cui, Angew. Chem. Int. Ed. 50 (2011) 7364–7368.
[5] X.L. Ji, K.T. Lee, L.F. Nazar, Nat. Mater. 8 (2009) 500–506.
[6] Y.Z. Fu, M. Arumugam, Chem. Mater. 24 (2012) 3081–3087.
[7] E. Ran, S. Gregory, G. Arnd, P. Alexander, A. Doron, Adv. Mater. 23 (2011) 5641–5644.
[8] S.-E. Cheon, K.-S. Ko, J.-H. Cho, S.-W. Kim, E.-Y. Chin, H.-T. Kim, J. Electrochem. Soc. 150 (2003) A796–A799.
[9] J. Wang, S.Y. Chew, Z.W. Zhao, S. Ashraf, D. Wexler, J. Chen, S.H. Ng, S.L. Chou, H.K. Liu, Carbon 46 (2008) 229–235.
[10] Y.V. Mikhaylik, J.R. Akridge, J. Electrochem. Soc. 151 (2004) A1969–A1976.
[11] L.X. Yuan, X.P. Qiu, L.Q. Chen, W.T. Zhu, J. Power Sources 189 (2009) 127–132.
[12] J. Hassoun, B. Scrosati, Angew. Chem. Int. Ed. 122 (2010) 2421–2424.
[13] G. Büchel, K.K. Unger, A. Matsumoto, K., Tsutsumi, Adv. Mater. 10 (1998) 1036–1038.
[14] W. Zheng, W.Y. Liu, X.G. Hu, C.F. Zhang, Electrochim. Acta 51 (2006) 1330–1335.
[15] C. Liang, N.J. Dudney, J.Y. Howe, Chem. Mater. 21 (2009) 4724–4730.
[16] J.C. Guo, Y.H. Xu, C.S. Wang, Nano Lett. 11 (2011) 4288–4294.
[17] Y.L. Cao, X.L. Li, I.A. Aksay, J. Lemmon, Z. Nie, Z.G. Yang, J. Liu, Phys. Chem. Chem. Phys. 13 (2011) 7660–7665.
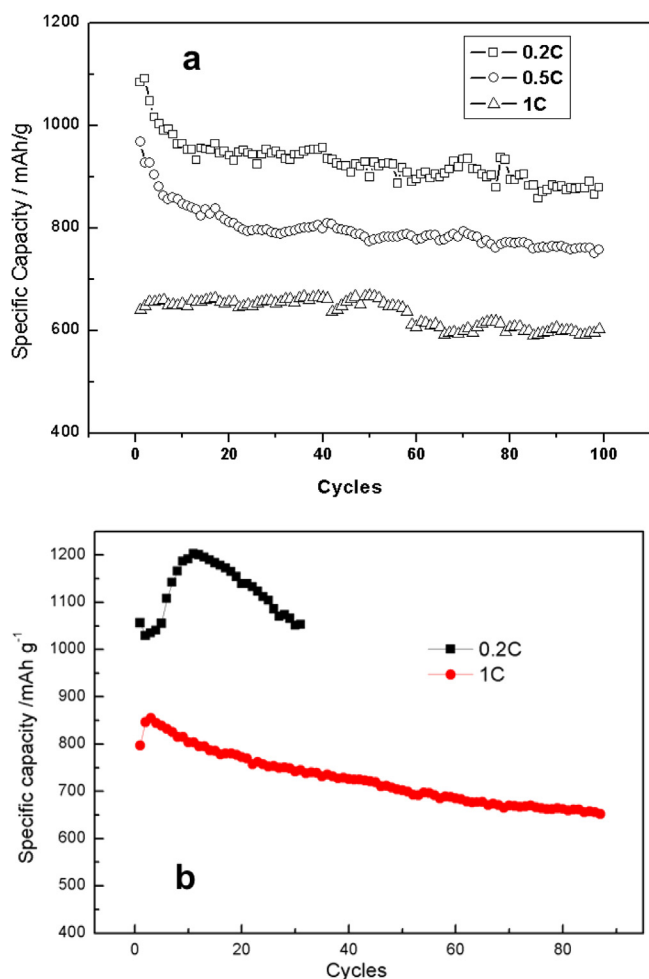[18] X.F. Wang, X.P. Fang, X.W. Guo, Z.X. Wang, L.Q. Chen, Electrochim. Acta 97 (2013) 238–243.

[19] J.W. Choi, J.K. Kim, G. Cheruvally, J.H. Ahn, H.J. Ahn, K.W. Kim, Electrochim. Acta 52 (2007) 2075–2082.
[20] L.R. Faulkner, U. Ill, I.J. Davidson, U.S. Patent 4, 752, 541, 1988.
[21] Z.Q. Jin, K. Xie, X.B. Hong, Z.Q. Hu, X. Liu, J. Power Sources 218 (2012) 163–167.
[22] H. Liang, X. Qiu, S. Zhang, W. Zhu, L. Chen, J. Appl. Electrochem. 34 (2004) 1211–1214.
[23] I. Gautier-Luneau, A. Denoyelle, J.Y. Sanchez, C. Poinsignon, Electrochim. Acta 37 (1992) 1615–1618.

[24] V.S. Kolosnitsyn, E.V. Karaseva, Russ. J. Electrochem. 44 (2010) 506.
[25] N. Jayaprakash, J. Shen, S.S. Moganty, A. Corona, L.A. Archer, Angew. Chem. Int. Ed. 50 (2011), 5904–5908.
[26] H. Schneider, A. Garsuch, A. Panchenko, O. Gronwald, N. Janssen, P. Novák, J. Power Sources 205 (2012) 420–425.
[27] V.S. Kolosnitsyn, E.V. Kuz'mina, E.V. Karaseva, S.E. Mochalov, Russ. J. Electrochem. 47 (2011) 793.
[28] Y.J. Choi, Y.D. Chung, C.Y. Beak, K.W. Kim, H.J. Ahn, J. Power Sources 184 (2008) 548.